



Published in final edited form as:

J Vasc Interv Radiol. 2010 June ; 21(6): 888–895. doi:10.1016/j.jvir.2009.12.402.

Electromagnetic Navigation for Thoracic Aortic Stent Graft Deployment: A Pilot Study in Swine

Nadine Abi-Jaoudeh, M.D.¹, Neil Glossop, PhD.⁴, Michael Dake, M.D.³, William F. Pritchard, M.D., PhD.², Alberto Chiesa, DVM., PhD.², Matthew R. Dreher, PhD.¹, Thomas Tang, PhD.⁴, John W. Karanian, PhD.², and Bradford J. Wood, M.D.¹

¹ Radiology and Imaging Sciences, National Institute of Health, Bethesda, MD

² Laboratory of Cardiovascular and Interventional Therapeutics, Center for Devices and Radiological Health, Food and Drug Administration, Laurel, MD

³ Department of Cardiothoracic Surgery Stanford University, CA

⁴ Traxtal Inc. Toronto ON, Canada

Abstract

Purpose—The goal of this study was to determine the feasibility of electromagnetic tracking as a method to augment conventional imaging guidance for the safe delivery, precise positioning, and accurate deployment of thoracic aortic endografts.

Materials & Methods—Custom guidewires were fabricated and the delivery catheters for thoracic aortic endoprostheses (Gore TAG endoprostheses, W.L. Gore & Assoc. Inc., Flagstaff AZ) were retrofitted with integrated electromagnetic coil sensors enabling realtime endovascular tracking. Pre-procedure thoracic CTA were obtained after placement of fiducial skin patches on the chest wall of three anesthetized swine, enabling automatic registration. The stent graft deployment location target near the subclavian artery was selected on the pre-procedure CTA. Two steps were analyzed: advancing a tracked glidewire to the aortic arch, and positioning the tracked stent graft assembly using electromagnetic guidance alone. Multiple CT scans were performed to evaluate the accuracy of the electromagnetic tracking system by measuring the target registration error which compared the actual position of the tracked devices to the displayed “virtual” electromagnetic-tracked position. Post-deployment CTA and necropsy confirmed stent graft position and subclavian artery patency.

Results—A stent graft was successfully delivered and deployed in each of the three animals using real-time electromagnetic tracking alone. The mean of the fiducial registration error of the auto-registration was 1.5 mm. Sixteen comparative scans were obtained to determine the target registration error, which was $4.3\text{mm} \pm 0.97\text{ mm}$ (Range: 3.0 to 6.0mm) for the glidewire sensor coil. The target registration error for the stent graft delivery catheter sensor coil was $2.6\text{ mm} \pm 0.7\text{ mm}$ (Range: 1.9 to 3.8 mm). The deployment error for the stent graft defined as deployment deviation from target was $2.6\text{mm} \pm 3.0\text{ mm}$.

Presentation: The following manuscript was presented at the SIR meeting in San Diego 2009.

The mention of commercial products, their source, or their use in connection with material reported herein is not to be construed as either an actual or implied endorsement of such products by the U.S. Food and Drug Administration, the National Institutes of Health, the Department of Health and Human Services or the Public Health Service.

Publisher's Disclaimer: This is a PDF file of an unedited manuscript that has been accepted for publication. As a service to our customers we are providing this early version of the manuscript. The manuscript will undergo copyediting, typesetting, and review of the resulting proof before it is published in its final citable form. Please note that during the production process errors may be discovered which could affect the content, and all legal disclaimers that apply to the journal pertain.

Conclusion—Delivery and deployment of customized thoracic stent grafts is feasible and accurate in swine using electromagnetic tracking alone. Combining endovascular electromagnetic tracking with conventional fluoroscopy may further improve accuracy and be a more realistic multi-modality approach.

Introduction

Thoracic aortic stent grafts have been approved for use in the US for the treatment of aneurysms in the thoracic descending aorta since 2005 (1). Their worldwide use for the treatment of transections, pseudoaneurysms, traumatic and non-traumatic dissections (2-4) has significantly grown over the past decade (2,3). This endovascular procedure is increasingly performed in the operating room with portable mobile C-arm fluoroscopy (3) which may not provide optimal imaging, especially in larger patients, and may lead to sub-optimal delivery and deployment.

Imaging feedback is essential for successful treatment since unintended coverage of the left subclavian artery may induce neurological symptoms requiring brachiocephalic revascularization (5,6). Improved methods to enhance visualization or navigation may be desirable to avoid these complications (2,4,7, and 8). Adequate delineation and localization of any dissection flap, differentiation between the true and false lumens or catheterization of the contralateral gate in cases of abdominal aortic aneurysm repair are essential steps (9). Therefore several angiograms in different views are often obtained to adequately position the device just prior to deployment. Although contrast induced nephropathy rarely occurs in individuals with normal renal function, the risk increases as much as 25% in unstable patients with renal disease (10), underlining the importance of contrast minimization during the procedure.

Electromagnetic navigation systems have been increasingly implemented in surgical applications (9,11). These navigation systems enable precise positioning and orientation of surgical, endoscopic, and interventional devices in patients, by referencing advanced imaging modalities usually not available in the procedure room. They can also be used to fuse pre- and intra-procedure imaging modalities such as ultrasound, MR, CT, and PET. Tracked needle placement is also increasingly used in percutaneous interventional oncology (12). Few publications are available however on the emerging technology of endovascular electromagnetic navigation. Early experiences with similar electromagnetic magnetically tracked wires and catheters in swine have been reported (12,13). Manstad-Hulaas (14) reported side-branched AAA stent graft insertion using navigation technology in phantoms. We performed an in vivo pilot study in 3 swine using electromagnetic navigation alone for thoracic stent graft deployment, with analysis of accuracy and feasibility.

Study Endpoints and Analysis

The purpose of the study was to determine whether electromagnetic tracking allows delivery and deployment of a modified thoracic aortic stent graft. Success was defined as accurate navigation and deployment of the stent graft as close as possible to a predetermined target vessel origin, without occluding or covering the vessel origin using electromagnetic navigation as sole source of guidance. Verification CTs and CTAs were performed to evaluate system accuracy for real time navigation of the customized devices i.e. tracked thoracic stent grafts. In each case, positioning of the stent graft was evaluated by pre and post deployment CTA as well as gross inspection at necropsy. A 2-3mm deviation from target was deemed acceptable. In a clinical setting with angiography, a 2mm deviation from the posterior wall of the subclavian artery would be difficult to assess. The fiducial registration error, target registration error and deployment error were assessed as explained below.

Definition of Measurements

The registration accuracy or “fiducial registration error” was assessed in each case by calculating the root mean square of the difference between the imaged position of the fiducial registration patches and their registered position in the electromagnetic field (15). The software automatically calculates this value, which is one measure of the quality of the registration.

Target registration error defines the error of mis-representation of the tracked device location reported by the system and its real location (and is due to the registration process). Target registration error is measured by determining the system-reported location of the tracked device (on the pre-procedural reference CT), and comparing it to the actual location of the same tracked device on a post manipulation CT image. To accurately determine target registration error, additional co-registrations, post-processing and calculations are required. The following calculations occurred as part of this study, and are not routinely acquired. Since it cannot be assumed that the pre-manipulation CT (initial) and post-manipulation CT scans are taken with the subject in the same location, it is necessary to co-register the pre-manipulation image (on which the navigation occurred) with the post-manipulation image that shows the device in a test location. Co-registration is performed by using the same fiducials registration patches (Figure 1) used for the initial registration (between subject space and image space) to register the pre and post-manipulation images, and determine the transformation between the pre- and post-image spaces. A co-registration matrix is calculated and used to transform the pre-manipulation data to the post-manipulation image, making it possible to depict the instrument location on the post manipulation scan, which also includes the actual location of the instrument; the target registration error is then calculated. Simplified, *the error distance* (target registration error) *is calculated between the electromagnetic sensor-displayed point and the actual point (as determined on the post-manipulation CT)*. The target registration error for all sensor coils was assessed, including the one at the tip of the guidewire and the sensor coil integrated in the delivery catheter at the level of the distal end of the stent graft. Note that determining the proximal tip location of the stent graft based on the sensor coil at the distal end of the latter is not ideal since the system assumes that the tip of the device lies in the same direction as the sensor and does not take into account bending between the sensor and the tip of the stent graft (See table 1 for more explanation).

Deployment error is defined as the difference between actual final stent graft position and the intended target deployment location. This is a systemic composite of registration, tracking, and operator errors, in addition to graft properties.

Methods and Materials

Swine Experimental Protocol

The non-survival procedures were performed under an approved Animal Use Protocol in compliance with federal regulations and NIH animal care standards. The normal swine weighed 104-124 lb. All procedures were performed under general anesthesia (Isoflurane), without paralytic drugs. The left jugular vein was accessed surgically and a 5Fr Avanti (Cordis Johnson & Johnson, Piscataway, NJ) sheath was placed. The right femoral artery was accessed surgically and a 6Fr Avanti (Cordis JnJ Piscataway, NJ) sheath was initially placed.

Hardware

Tracked guidewires and stent grafts were custom fabricated and retrofitted with integrated embedded sensor coils (Traxtal Inc, Toronto, Ontario). Custom hydrophilic-coated angled guidewires were fabricated (Traxtal Inc, a Philips Healthcare Company, Toronto, Ontario) with an internal sensor coil at the tip. Thoracic aortic Endoprostheses, (Gore TAG endoprostheses, W.L. Gore & Associates Inc., Flagstaff, AZ) were retrofitted with a micro-sensor coil at the

distal end of the stent extending along the delivery catheter shaft (Figure 2). All stent grafts were 26mm in diameter \times 10cm in length.

Navigation Technology and Software

The navigation system is an experimental, custom modified, endovascular software derived of a commercially marketed image guided intervention system (Traxtal Inc.) The system uses a small electromagnetic field generator (Aurora; Northern Digital, Waterloo, Ontario) placed on a modified passive support and positioning arm. The generator produces an ultra-low electromagnetic field ($<70\mu\text{T}$) enabling simultaneous tracking of the several sensor coils within a work volume of 500mm \times 500mm \times 500mm. A weak current is induced within the sensor coil that is converted to the coil's location and orientation relative to the electromagnetic field generator. Once registered, the position of any tracked device within the work volume will be projected in real time onto the CT images as a graphic icon superimposed on the images.

Experiment Description

Three attached automatic registration patches (Traxtal Inc.) were positioned on the least mobile part of the chest; the sternum and ribs (Figure 1). These fiducial registration patches are radio-opaque and are actively tracked so they can partly correct for respiratory motion alterations and gross motion of the subject. A CT angiogram of the thoracic aorta (that included the patches) was obtained in arterial phase following an intravenous injection of iodinated non-ionic contrast (Iovue 300, Bracco, Princeton, NJ, USA) at 1mL/Kg at a rate of 2ml/sec on a 16 detector row CT (MX8000/IDT, Philips Medical Systems, Cleveland, OH) with 2 mm slice thickness and 1 mm spacing. Breath-hold was achieved by mechanically fully inflating the lungs of the pigs (2kPa), without use of paralytic agents. All CT scans were performed with breath-hold. The pre-CTA with the fiducial patches in place allowed for automatic registration once transferred to the navigation software and partly corrected for respiratory motion. The fiducial registration error was recorded for each procedure after that initial CTA. The deployment target site, the aortic arch immediately posterior to the origin of the left subclavian artery was also selected on the navigation software display. Therefore the target was marked on the reformatted images of the CTA in all 3 planes and the 3D view.

A tracked guidewire was advanced from the common femoral artery access to the aortic arch using electromagnetic tracking. The tracked wire is projected on the reformatted CT images in all 3 planes as two crossing yellow lines. As the operator advances the wire, the position of the two crossing yellow lines (representing the wire), changes (See figure 3 and 4).

The target registration error for the wire was determined by navigating the wire and catheter to the vicinity of a great vessel origin (used as a landmark on imaging) with electromagnetic tracking. The "virtual" location coordinates of the tracked wire were recorded and a non-enhanced thoracic CT with 2 mm slice thickness and 1 mm spacing was obtained simultaneously in order to compare the actual location of the guidewire on imaging with the "virtual" or tracked location. The operator was blinded to the results of the CT scan to insure that navigation and deployment were performed with electromagnetic guidance alone. This process was repeated several times to obtain several target registration error measurements. Of note some target registration error measurements were obtained with the tracked tool advanced into a great vessel while others were obtained with the tracked tool in the aorta adjacent to the origin of a great vessel.

Once the tracked hydrophilic guidewire was exchanged for a stiff Amplatz guidewire, the graft sheath was inserted from the groin. The stent graft was then advanced into the descending aorta from the common femoral artery access. Using the electromagnetic tracking system alone, the stent graft assembly was positioned. The position of the sensor coil used for navigation is

displayed real time in all 3 planes and 3D view in reformatted images of the initial CTA. Additional non-enhanced thoracic CTs with 2 mm slice thickness and 1 mm spacing, were obtained for additional target registration error measurements of the stent graft shaft sensor coil. The stiff Amplatz guidewire was then exchanged for the tracked hydrophilic guidewire placed at the tip of the stent graft. Additional target to registration error measurements were obtained with the tracked hydrophilic guidewire sensor coil. The operator remained blinded to these CT results. Following the CT for error measurement, the stent graft was deployed at the predetermined target, just distal to the posterior wall of the subclavian artery. A post-deployment CTA of the thorax was obtained with the same field of view and conditions used for the pre-deployment CTA to confirm adequate stent graft placement and subclavian patency. While under general anesthesia, euthanasia was performed by exsanguination followed by necropsy. At that time, two separate operators measured the distance from the leading edge of the stent graft to the origin of subclavian artery. A total of sixteen CTs were obtained for target registration error measurements throughout the procedures, nine for the glidewire sensor coil and seven for the stent graft coil. Nine, four and three CT scans were performed in the first, second and third subject cases, respectively.

Results

General outcome of procedures

Three modified thoracic aortic endoprostheses (Gore TAG endoprostheses, W.L. Gore & Associates Inc, Flagstaff, AZ, USA) were successfully delivered and deployed in three swine using electromagnetic tracking, without fluoroscopic guidance. The operator was blinded to the results of all CT-scans except the initial pre-deployment CTA, which was loaded onto the navigation system and used to determine the target site and catheter guidance. Electromagnetic tracking enabled accurate display with real time updating of the wire and stent graft positions displayed on previously acquired imaging datasets. Both the wire and stent graft were successfully navigated with electromagnetic tracking into the aortic arch and descending aorta respectively. The wire was also successfully navigated with electromagnetic tracking into the branches of the arch vessels such as the left subclavian artery and left carotid artery.

Procedure time and contrast dose

The average procedure time was 240 minutes \pm 80 minutes. The average contrast load was 158 mL \pm 38 mL per case (including pre- and post-deployment CTA as well as a pelvic CTA in the first case to assure proper sizing of the introducer sheath).

Results of measurements obtained

The error between displayed and the actual positions of electromagnetic tracked stent graft system components were obtained (table 2). The fiducial registration error was 1.5mm. The target registration error with the sensor-enabled glidewires was 4.3mm \pm 0.9mm (range 3.0mm-6.0mm). The target registration error of the tip of the stent graft using the glidewire sensor coil was 4.4 mm \pm 0.4 mm (Range: 4.0 mm - 4.9 mm). The target registration error of the stent graft shaft coil itself was 2.6 mm \pm 0.7 mm (Range: 1.9 mm - 3.8 mm). However estimating and projecting the distal tip of the stent graft using the sensor coil on the stent graft delivery catheter had a target registration error of 8.8 mm \pm 2.4 mm (Range 6.8 mm - 12.6 mm). Similarly obtaining the target registration error of the position of the distal end of the stent graft using the glidewire placed at the proximal tip of the stent graft was 9.2 mm \pm 2.5mm (Range: 5.7mm - 11.5 mm).

In the second case, the fiducial registration error and an initial set of target registration error measurements (two target registration errors for the glidewire sensor coil and one for the stent graft sensor coil) were excluded due to metal interaction caused by the physical proximity of

an unused nearby C-arm image intensifier. Moving the image intensifier solved the metal interaction inaccuracy problem, and repeat fiducial registration error and target registration error measurements were successfully performed. Moreover during that same case (swine 2), we were unable to obtain target registration error measurements of the stent graft position using the glidewire coil, due to a known defect in the stent graft, preventing exchange of a stiff wire for a tracked glidewire.

The deployment error or difference between actual final stent graft position and the target location according to the post-deployment CTA (Figure 5) was $2.6 \text{ mm} \pm 3.0 \text{ mm}$ (Range: 0-5.9 mm). The deployment error on gross examination at necropsy was concordant with the CTA measurements as determined by two independent observers (Figure 6).

Discussion

Multimodality imaging and navigation in endovascular interventions is now translatable to clinic, with the emergence of fusion CT and angiography tables, MRI and angiography tables, rotational fluoroscopy/cone-beam CT, and electromagnetic tracking hardware and software (16-18). Endovascular devices enabled with medical GPS-like positioning and tracking technology allow the interventional operator to reference pre-procedural imaging in real time. Such technology can bring multiple modalities together in different combinations and timing, when clinically needed (11-13) to procedural areas normally devoid of this information. Stent graft deployment is one possible clinical application for this paradigm. The three-dimensional perspective obtained with electromagnetic navigation may provide a substantial contribution in cases of dissections (19-24) by facilitating differentiation of the true and false lumens. It may also improve volumetric localization of the contralateral gate in abdominal aortic repair, and can potentially offer valuable input with fenestrated/ side branched aortic grafts (14).

Electromagnetic tracking for endovascular procedures may include directly integrated hardware, in order to take advantage of potential improvement in accuracy, decreased contrast, time or radiation. The contrast usage reported in this study included additional contrast used for verification CTAs, which would not normally be required during an actual procedure since only an angiogram would be obtained post deployment. The pre-procedure CTA or MRA may actually be acquired hours or days prior to the deployment procedure as part of the pre-procedural evaluation (26), further decreasing peri-procedural risk for acute tubular necrosis.

The system's performance is measured as the target registration error and especially the deployment error. The distance between the sensor coil and the point to be tracked affected the target registration error. For example if the tracked wire is positioned at the tip of the delivery catheter, then the target registration error for the delivery catheter tip using the sensor coil on the wire may be clinically acceptable. However the target registration error of the wire's sensor coil will not be clinically acceptable if the wire is leading and free floating in the aorta. It is conceivable to consider that the tracked wire can move with aortic pulsations during a CT scan. If the sensor coil moves with a pulsation a few mm lateral and a few mm below its position on the snap shot taken by the navigation system, then the target registration error will be the square root of the sum of the distance difference in each plane; however this is not clinically relevant. In other words, the wire/stent graft did not advance or get pulled back; rather they simply floated in a large pulsating vessel, the aorta. Thus the target registration error tends to exaggerate the system's inaccuracy in the pulsing vascular system. Again if the tracked tool is advanced into a great vessel where motion is reduced then the target registration error will be diminished hence explaining the variation between the target registration error measurements obtained with the same sensor coil. Moreover, if the sensor coil at the distal end of the graft is used to estimate the position of the tip of the stent, the target registration error will be even larger. Indeed not only is the tip of the stent floating in the aorta but also the calculations based

upon a remote sensor coil will estimate and project the tip of the stent without accounting for bending. Therefore placing the sensor on the device, at the exact location to be tracked is most reliable.

The deployment error, representing the final position of the stent graft compared to its desired location is the most important element. In the present study the electromagnetic system alone allowed accurate deployment of the stent graft near the target site (2.6mm deployment error).

Although this study demonstrated the feasibility of stent graft deployment with electromagnetic guidance alone, electromagnetic navigation will not replace fluoroscopy, but rather may augment existing paradigms. Similar to electromagnetic ultrasound and CT fusion applications in interventional oncology, the vascular operator will likely have simultaneous access to the multimodality imaging feedback as well as the conventional fluoroscopic imaging. Recent technical developments have enabled integration of tracking technology directly into fluoroscopy flat detector systems without the interference caused by metallic components of an image intensifier based system (25).

Future studies will assess accuracy in a clinical trial setting for endovascular devices, as well as address integration hurdles related to electromagnetic interactions with conventional and flat detector fluoroscopic systems.

Acknowledgments

This work is supported in part by the Intramural Research Program of the NIH. This project is a collaboration between the National Institute of Health (NIH) and the Food and Drug Administration (FDA) as part of an interagency agreement. We thank W.L. Gore Flagstaff, Arizona, USA for the donation of the TAG devices. We would also thank Julia Locklin for her contributions to the illustrations and image processing.

References

1. Svensson LG, Kouchoukos NT, Miller DC, et al. Expert consensus document on the treatment of descending thoracic aortic disease using endovascular stent-grafts. *Ann Thorac Surg* 2008;85:S1–41. [PubMed: 18083364]
2. Tiesenhausen K, Hausegger KA, Oberwalder P, et al. Left subclavian artery management in endovascular repair of thoracic aortic aneurysms and aortic dissections. *J Card Surg* 2003;18:429–435. [PubMed: 12974933]
3. Schumacher H, Bockler D, von Tengg-Kobligk H, Allenberg JR. Acute traumatic aortic tear: open versus stent-graft repair. *Semin Vasc Surg* 2006;19:48–59. [PubMed: 16533692]
4. Weigang E, Luehr M, Harloff A, et al. Incidence of neurological complications following overstenting of the left subclavian artery. *Eur J Cardiothorac Surg* 2007;31:628–636. [PubMed: 17275319]
5. Noor N, Sadat U, Hayes PD, Thompson MM, Boyle JR. Management of the left subclavian artery during endovascular repair of the thoracic aorta. *J Endovasc Ther* 2008;15:168–176. [PubMed: 18426279]
6. Hodgson KJ, Matsumura JS, Ascher E, et al. Clinical competence statement on thoracic endovascular aortic repair (TEVAR)--multispecialty consensus recommendations. A report of the SVS/SIR/SCAI/SVMB Writing Committee to develop a clinical competence standard for TEVAR. *J Vasc Surg* 2006;43:858–862. [PubMed: 16616253]
7. Fattori R, Nienaber CA, Rousseau H, et al. Results of endovascular repair of the thoracic aorta with the Talent Thoracic stent graft: the Talent Thoracic Retrospective Registry. *J Thorac Cardiovasc Surg* 2006;132:332–339. [PubMed: 16872959]
8. Nienaber CA, Kische S, Ince H. Thoracic aortic stent-graft devices: problems, failure modes, and applicability. *Semin Vasc Surg* 2007;20:81–89. [PubMed: 17580245]
9. Kaspersen JH, Sjolie E, Wesche J, et al. Three-dimensional ultrasound-based navigation combined with preoperative CT during abdominal interventions: a feasibility study. *Cardiovasc Intervent Radiol* 2003;26:347–356. [PubMed: 14667116]

10. Morcos SK. Prevention of contrast media-induced nephrotoxicity after angiographic procedures. *J Vasc Interv Radiol* 2005;16:13–23. [PubMed: 15640403]
11. Schichor C, Witte J, Scholler K, et al. Magnetically guided neuronavigation of flexible instruments in shunt placement, transsphenoidal procedures, and craniotomies. *Neurosurgery* 2008;63:ONS121–127. discussion ONS127-128. [PubMed: 18728589]
12. Wood BJ, Zhang H, Durrani A, et al. Navigation with electromagnetic tracking for interventional radiology procedures: a feasibility study. *J Vasc Interv Radiol* 2005;16:493–505. [PubMed: 15802449]
13. Levy EB, Zhang H, Lindisch D, Wood BJ, Cleary K. Electromagnetic tracking-guided percutaneous intrahepatic portosystemic shunt creation in a swine model. *J Vasc Interv Radiol* 2007;18:303–307. [PubMed: 17327566]
14. Manstad-Hulaas F, Ommedal S, Tangen GA, Aadahl P, Hernes TN. Side-branched AAA stent graft insertion using navigation technology: a phantom study. *Eur Surg Res* 2007;39:364–371. [PubMed: 17664876]
15. Frantz DD, Wiles AD, Leis SE, Kirsch SR. Accuracy assessment protocols for electromagnetic tracking systems. *Phys Med Biol* 2003;48:2241–2251. [PubMed: 12894982]
16. Tam A, Mohamed A, Pfister M, Rohm E, Wallace MJ. C-arm Cone Beam Computed Tomographic Needle Path Overlay for Fluoroscopic-Guided Placement of Translumbar Central Venous Catheters. *Cardiovasc Intervent Radiol*. 2009
17. Raman VK, Lederman RJ. Advances in interventional cardiovascular MRI. *Curr Cardiol Rep* 2006;8:70–75. [PubMed: 16507240]
18. Omary RA, Gehl JA, Schirf BE, et al. MR imaging- versus conventional X-ray fluoroscopy-guided renal angioplasty in swine: prospective randomized comparison. *Radiology* 2006;238:489–496. [PubMed: 16436813]
19. Dake MD, Wang DS. Will stent-graft repair emerge as treatment of choice for acute type B dissection? *Semin Vasc Surg* 2006;19:40–47. [PubMed: 16533691]
20. Marcheix B, Dambrin C, Bolduc JP, et al. Endovascular repair of traumatic rupture of the aortic isthmus: midterm results. *J Thorac Cardiovasc Surg* 2006;132:1037–1041. [PubMed: 17059920]
21. Semba CP, Kato N, Kee ST, et al. Acute rupture of the descending thoracic aorta: repair with use of endovascular stent-grafts. *J Vasc Interv Radiol* 1997;8:337–342. [PubMed: 9152904]
22. Orend KH, Pamler R, Kapfer X, Liewald F, Gorich J, Sunder-Plassmann L. Endovascular repair of traumatic descending aortic transection. *J Endovasc Ther* 2002;9:573–578. [PubMed: 12431137]
23. Rousseau H, Dambrin C, Marcheix B, et al. Acute traumatic aortic rupture: a comparison of surgical and stent-graft repair. *J Thorac Cardiovasc Surg* 2005;129:1050–1055. [PubMed: 15867779]
24. Yang J, Zuo J, Yang L, et al. Endovascular stent-graft treatment of thoracic aortic dissection. *Interact Cardiovasc Thorac Surg* 2006;5:688–691. [PubMed: 17670684]
25. Racadio JM, Babic D, Homan R, et al. Live 3D guidance in the interventional radiology suite. *AJR Am J Roentgenol* 2007;189:W357–364. [PubMed: 18029850]
26. Bean MJ, Johnson PT, Roseborough GS, Black JH, Fishman EK. Thoracic aortic stent-grafts: utility of multidetector CT for pre- and postprocedure evaluation. *Radiographics* 2008;28:1835–1851. [PubMed: 19001643]

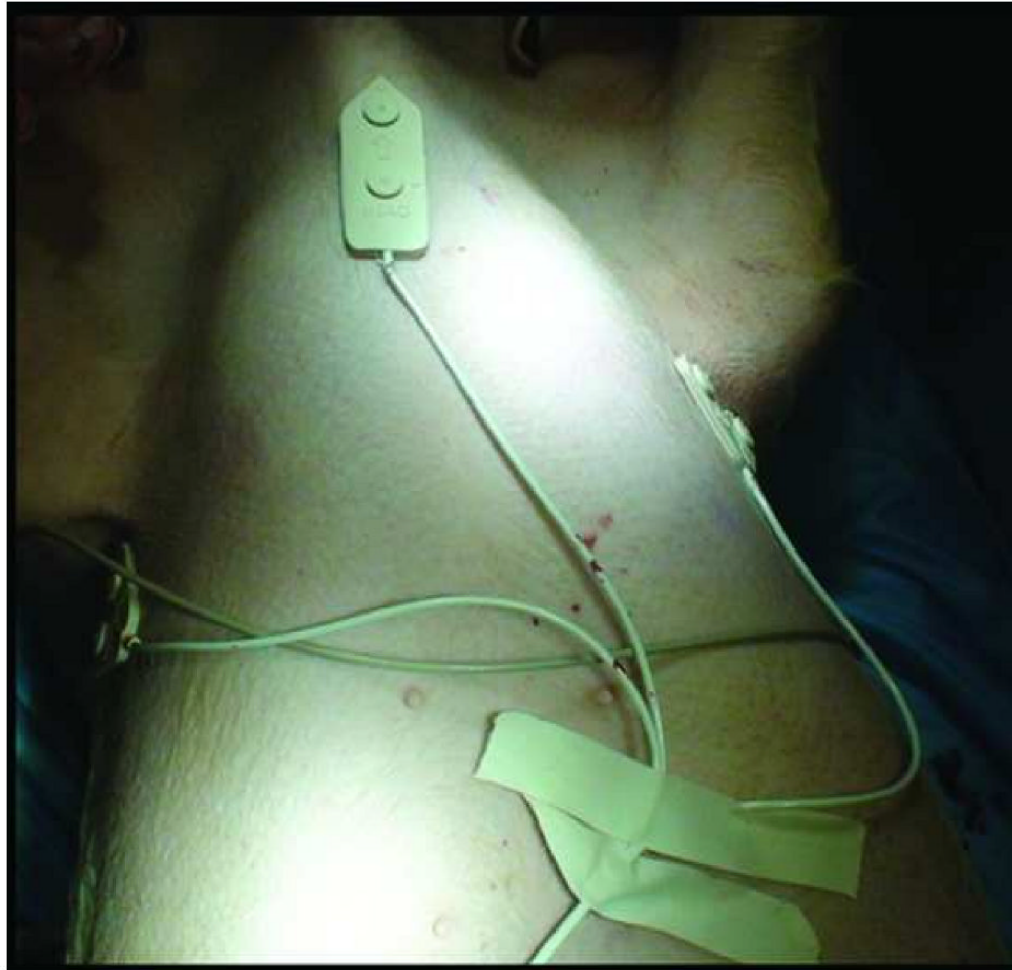


Figure 1. Fiducial registration patches allow automatic registration. Three fiducial registration patches (white patch with arrow) were placed on immobile part of the swine chest; the ribs and sternum.



Figure 2. TAG device with integrated sensor coil. The arrow highlights the location of the sensor coil with the wire extending along its delivery catheter shaft.

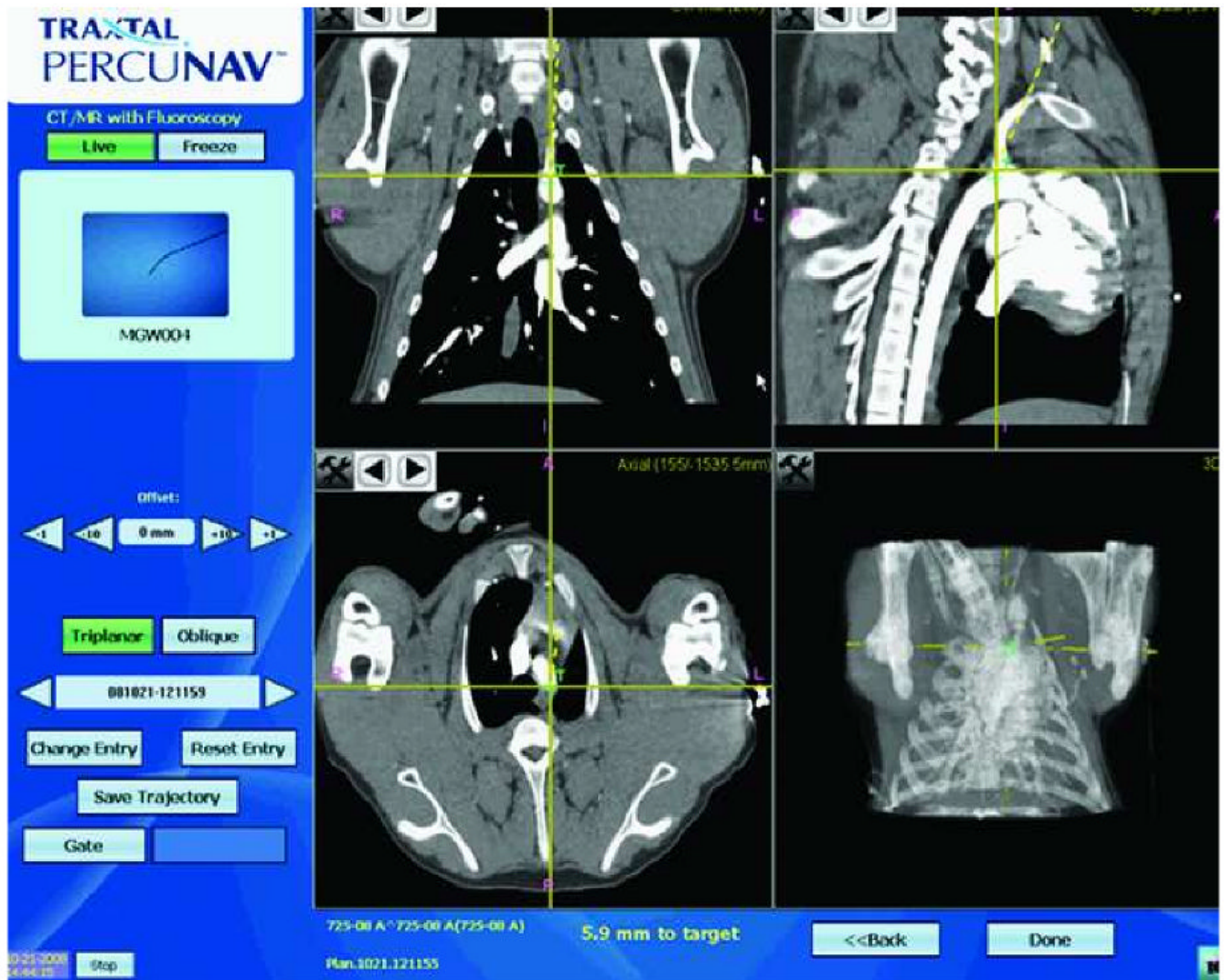


Figure 3. Graphical user interface for electromagnetic-guided navigation. The screen display (Traxtal Inc., Toronto) shows the tracked tool (left upper corner), in this case an angled guidewire (large black arrow). The yellow crossing lines on each panel indicate the position of the tracked sensor coil. The target “T” is displayed as a small green cross on the pre-procedure CTA. Each panel shows the position of the tracked tool in relation to target in one of the three planes, sagittal, coronal and axial as well as a 3D view. The dotted yellow line indicates the direction the tracked tool. The distance to the target in mm is also shown at the bottom of the screen. The position and orientation of the tracked tool and the distance to target is updated real time.

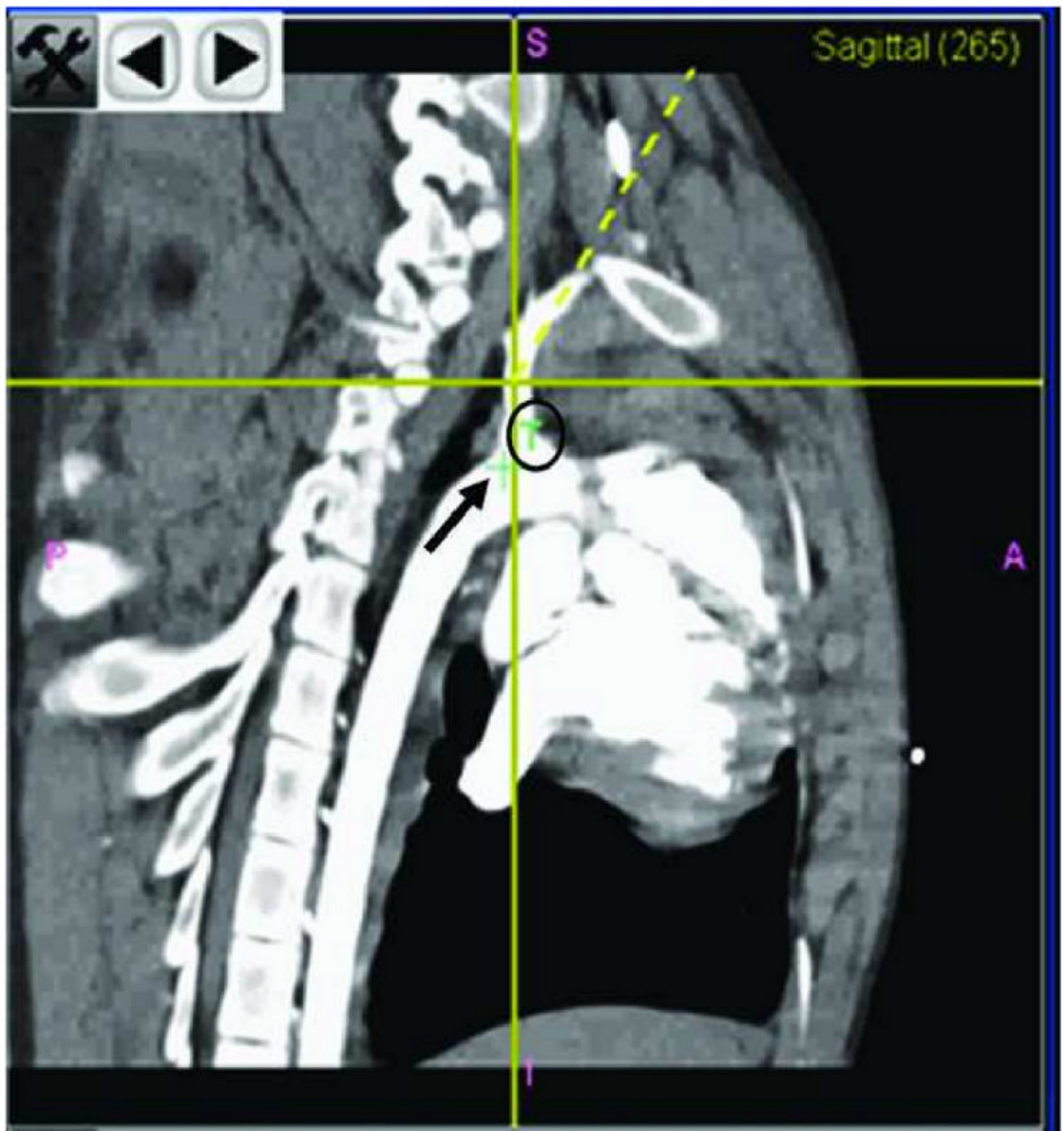


Figure 4.

Panel B is enlarged. It displays the position of the tracked tool in the sagittal plane. The small green cross (black arrow) is the actual position of the target. The "T" (black circle) explains the significance of the small green cross. The yellow crossing lines indicate the position of the tracked tool. The yellow dotted line is the direction of the tracked tool.



Figure 5. 2D MIP Reconstruction of a contrast enhanced CT of the thoracic aorta post-deployment demonstrates the position of the stent graft in relation to the subclavian artery. The deployment catheter is still in place when the CTA was taken.

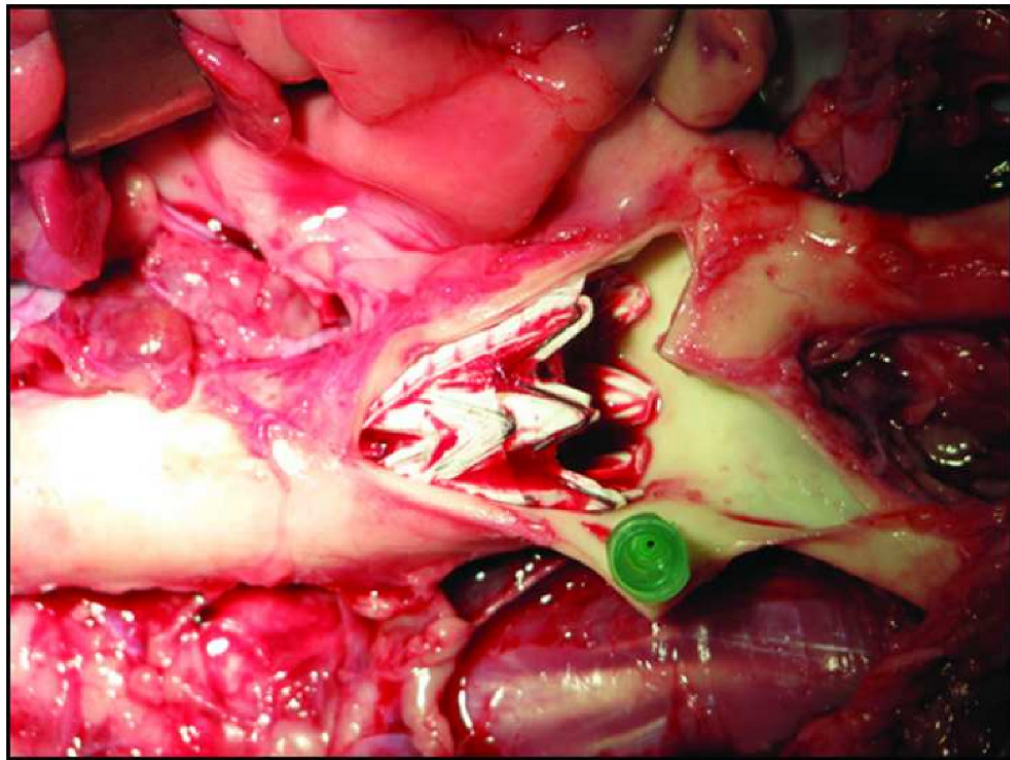


Figure 6. Gross dissection of thoracic aorta and subclavian artery post necropsy. The position of the stent in close proximity to the subclavian artery origin has been marked by a needle (green).

Table 1

Definition of measurements.

Name	Significance	Method of Calculation
Fiducial Registration error	Registration accuracy Assessment obtained in every case	The Fiducial registration error is the root-mean square of the distance between the localized position of each fiducial as transformed from image space to physical space and the position of that corresponding fiducial localized in physical space.
Target Registration error	Misrepresentation of the tracked device location by the navigation system as opposed to actual position on imaging	The tracked device is placed at a target and its location (x, y, z) is recorded immediately prior to obtaining a verification CT-scan. The navigation CT scan is co-registered to the verification scan and the recorded location of the tracked device is transformed into the verification scan space. The distance between the position of the tracked device now depicted on the verification scan and the actual image of the tracked device provides the target registration error.
Deployment error	Overall accuracy of system	Sum of all errors including fiducial registration error, target registration error, operator error and graft properties

Table 2

The target registration error between displayed and actual positions of tracked components in mm

	TRE of the GW tip	TRE at the proximal end of the stent using GW coil	TRE at the distal end of the stent using GW coil	TRE at distal end of the stent using stent coil	TRE at the proximal end of the stent using shaft coil
Mean	4.3	4.4	9.2	2.6	8.8
STDEV	0.9	0.4	2.5	0.7	2.5
Min	3.0	4.0	5.7	1.9	6.8
Max	6.0	4.9	11.5	3.8	12.6

TRE: Target Registration Error

STDEV: standard deviation

GW: glidewire